Measuring the optical properties of astrophysical dust analogues: instrumentation and methods

Stephen A. Rinehart,[1,*] Dominic J. Benford,[1] Giuseppe Cataldo,[1,†] Eliahu Dwek,[1] Ross Henry,[2] Raymond E. Kinzer, Jr.,[1,§] Joseph Nuth,[3] Robert Silverberg,[1] Caleb Wheeler,[4] and Edward Wollack[1]

[1]NASA's Goddard Space Flight Center, Code 665, Greenbelt, Maryland 20771, USA

[2]NASA's Goddard Space Flight Center, Code 551, Greenbelt, Maryland 20771, USA

[3]NASA's Goddard Space Flight Center, Code 693, Greenbelt, Maryland 20771, USA

[4]Arizona State University, Tucson, Arizona 85287, USA

*Corresponding author: Stephen.A.Rinehart@nasa.gov

Received 13 April 2011; revised 9 June 2011; accepted 10 June 2011;
posted 14 June 2011 (Doc. ID 145226); published 19 July 2011

Dust is found throughout the universe and plays an important role for a wide range of astrophysical phenomena. In recent years, new IR facilities have provided powerful new data for understanding these phenomena. However, interpretation of these data is often complicated by a lack of complementary information about the optical properties of astronomically relevant materials. The Optical Properties of Astronomical Silicates with Infrared Techniques (OPASI-T) program at NASA's Goddard Space Flight Center is designed to provide new high-quality laboratory data from which we can derive the optical properties of astrophysical dust analogues. This program makes use of multiple instruments, including new equipment designed and built specifically for this purpose. The suite of instruments allows us to derive optical properties over a wide wavelength range, from the near-IR through the millimeter, also providing the capability for exploring how these properties depend upon the temperature of the sample. In this paper, we discuss the overall structure of the research program, describe the new instruments that have been developed to meet the science goals, and demonstrate the efficacy of these tools.

OCIS codes: 120.3150, 120.4530, 120.4570.

1. Introduction

For over four decades, it has been known from IR observations that silicates are present in a variety of different astrophysical environments [1,2]. Early photometric observations showed a broad IR excess at both 10 and 20 μm; these excesses were well explained by theoretical predictions of the IR spectra of silicate-rich minerals such as olivine [$(Mg, Fe)_2SiO_4$].

For several decades after the identification of the 10 μm silicate feature, photometry and low-resolution spectroscopy from the ground were the only tools available for exploring the IR universe. With the advent of powerful new space-based observatories, high-resolution spectroscopy and access to a much wider spectral range in the far-IR has revealed a wide array of broad spectral features (e.g., with the Infrared Space Observatory (ISO), [3]). Many of these broad features appear in conjunction with the 10 μm silicate feature, leading astronomers to conclude that the broad features at long wavelengths are attributable to the presence of silicate-rich dust. Unfortunately, interpretation of these data has been hampered by the limited laboratory data available. Attempts to fit the observed spectra using laboratory

0003-6935/11/214115-09$15.00/0

data obtained with terrestrial minerals (e.g., forsterite, enstatite) show that while these minerals can explain some of these observed features, they fall short of being able to self-consistently account for all of the observed IR features.

Several possible explanations exist for the discrepancy. First, astronomical dust is likely an amalgam of a number of unique materials, with different individual substances dominating at different wavelengths. By using a linear combination of the spectra from different silicate-rich minerals, astronomers have had greater success in matching observations, but they still face inconsistencies when trying to match features across a wide range of wavelengths [4]. A second explanation is that terrestrial minerals are actually poor analogues to astronomical silicates and that the spectra of such minerals are fundamentally different from the spectra of astronomical dust. In the unprocessed state, silicate grains are referred to as "amorphous." However, virtually all laboratory spectra of "amorphous" material in the astrophysical literature are those of glassy solids [5,6]. Such material is relatively easy to make in large quantities, and laboratory measurements of these samples provide a reasonable first approximation to astrophysical dust. It is possible, however, to produce materials that are better analogues to astrophysical dust; measurements of such samples are needed to complement and interpret the high-quality IR spectroscopic data now being produced.

Consider the formation of dust in the astronomical environment. In regions of dust formation (e.g., outflows from late-type stars), a hot gas is expelled from the star. Within this gas are the fundamental constituents of dust, including water and metals. As the gas cools, it begins to condense; the condensate that forms out of the gas is chaotic and disordered, bearing little or no resemblance to the well-ordered crystalline structures found within terrestrial minerals. This condensate is the most basic (amorphous) type of silicate dust and is commonly found in new, relatively unprocessed dust. However, astronomical observations also imply the presence of crystalline silicates in regions where the dust has been processed. Such processing typically happens through annealing of the dust grains, as exposure to high temperatures causes the condensate to gain order and become more crystalline. The annealing process has been demonstrated via a very simple, yet elegant, experiment. Amorphous magnesium silicate condensates were placed on a heated stage within a transmission electron microscope, and physical changes in the grain were monitored as a function of temperature and time [7]. After sufficient annealing, a thin layer of interconnected crystalline nuclei can form on the surface of the amorphous dust grain, but with no crystals within the grain interior; continued annealing causes the crystal nuclei to grow toward the center of the grain, first forming a multicrystalline solid, then fusing into a single crystal grain. These latter two stages are extremely rare in astrophysical environments, if they exist at all under such conditions.

While laboratory experiments have provided data for glassy samples, very little data exist for the chaotic condensates that best represent the majority of the silicates that are more commonly found in astronomical environments. Such materials have been manufactured, but laboratory data of the optical constants have only been acquired over a limited spectral range and only at room temperature [8]. The optical properties of silicate dust grains at low temperatures have long been known to differ from those at room temperature [9,10]. Recent work has shown that these spectral changes are more significant than perhaps previously thought, with changes in both position and shape of spectral features and in the underlying continuum opacity [11]. However, such measurements have only been made at a very limited number of temperatures. More complete temperature sampling in such experiments may enable astronomers to use astronomical spectra of dust as a direct temperature diagnostic.

The Optical Properties of Astronomical Silicates with Infrared Techniques (OPASI-T) program is designed to provide new laboratory data over a wide wavelength range and a wide range of sample temperatures. These data allow calculation of the complex dielectric constants and optical constants, providing key information necessary to help us understand physical processes in astronomical environments. In this paper, we discuss the overall formulation of the OPASI-T program and show data that demonstrate the efficacy of the different instruments and techniques.

2. Overview of the OPASI-T Program and Methodology

Previous and ongoing laboratory astrophysics programs have provided measurements for different types of materials (see [12] for a review). Much of this work is based upon measurements of macroscopic mineral solids ground into fine particles [5,6]. The disadvantage of this method, whether the solid used is crystalline or in a melt form of the mineral, is that the grains produced are highly ordered at the molecular level compared to the amorphous condensates produced in astronomical environments. Another method, the sol-gel technique, produces dust grains that are more representative of astronomical dust grains, in that these particles are amorphous in chemical content and structure, but unlike the chaotic condensates often found in astronomical environments, they still contain silicate tetrahedral monomers. Further, the grains produced by the sol-gel method tend to be small and relatively uniform in shape and structure. This is in contrast to the observed structure of interplanetary grains, where microscopy shows a complicated, almost fractal, structure. The structure itself can have noticeable effects on the observed spectrum of grains [13]. Laser ablation, arc-discharge ablation, and smoke

condensation are new methods that can better reproduce the amorphous chemistry and the complicated morphology of astronomical dust grains [14]. We produce samples using the smoke condensation method [8], which also produces a relatively uniform particle size.

To take full advantage of the high quality of our samples and to provide the range of laboratory data needed to properly interpret astronomical spectra, our laboratory astrophysics program is designed to address two major challenges. The first challenge is providing the wide range of wavelength coverage, from the mid-IR through the millimeter, needed to match the state-of-the-art capabilities of astronomical facilities such as *Spitzer*, *Herschel*, SOFIA, and ALMA. Individual measurement methods (e.g., bulk measurements, matrix methods) provide access to different spectral ranges, but no one method provides sufficiently broad wavelength coverage. This leads the OPASI-T program to use several different sample preparation methods, providing broad spectral coverage. Transmission data are acquired in the mid- to far-IR using a Fourier transform spectrometer (FTS). Matrix samples (suspensions) provide coverage at short wavelengths, while bulk samples provide access at long wavelengths. However, transmission data alone do not uniquely determine the fundamental optical constants that one would like to derive. Also needed are either absorption or scattering measurements of the samples. We obtain scattering data (and absorption data) for our samples using a new instrument developed under OPASI-T: an IR reflectometer.

At long wavelengths (>800 microns), we use waveguide techniques developed for measuring material properties in the millimeter regime. This technique is ideal in that it provides direct measurement of the complex dielectric constant. However, this technique only works at long wavelengths, where the samples appear essentially homogenous with a high degree of flatness, parallelism, and specular reflection.

The second challenge is temperature control of the sample. Recent experiments have shown that the spectral features from silicate-rich materials can vary significantly as a function of temperature, with changes in the strength, shape, and position of spectral features [11]. Unfortunately, the measurements to date have been limited; at most, measurements have only been taken at room temperature and liquid nitrogen and liquid helium temperatures, and in all cases, the spectral range of these temperature-dependent measurements has been very limited (only wavelengths $<100\,\mu$m). While the limited temperature coverage shows variation in the observed spectral features, it does not allow determination of where (in temperature) these changes begin and end. Measurements with additional temperature resolution are needed if we are to understand the functional dependence of the spectrum upon temperature, although very fine temperature resolution is not strictly necessary. Unless the dust materials exhibit a rapid change of properties at some temperature (e.g., a phase change), relatively low resolution is sufficient for understanding astronomical data, since the spectrum should change smoothly and slowly as a function of temperature. Therefore, the OPASI-T program apparatus are designed to allow for measurements over a wide range of temperatures and over a broad spectral range.

3. Instrumentation

Early results from the OPASI-T program have been presented previously in several conference proceedings [15,16]. In this section we present details on the instruments and techniques that comprise this effort.

A. Fourier Transform Spectrometer—Transmission Measurements

We require an array of different sample preparation techniques to provide the wide range of wavelength coverage. These fall into two categories: the sample embedded in a matrix and bulk samples. The difficulty with bulk-sample methods is that in order to create a homogenous sample, one needs to use a relatively large quantity of the sample material. This leads to high optical depths ($\tau > 1$) in the near- and mid-IR, making accurate transmission and absorption measurements impossible due to saturation. In the far-IR, where the grain opacity drops, these bulk samples remain optically thin while providing sufficient depth to allow measurements.

Conversely, matrix methods work well in the near- and mid-IR. Relatively small amounts of sample material can be embedded in a matrix material such as KBr, CsI, or polyethylene. The filling fraction of the sample material is set when the sample pellet is produced. By using a small amount of sample material, the sample remains optically thin at short wavelengths, allowing accurate measurement of transmission and absorption. At longer wavelengths, the optical depth decreases, and as the transmission approaches unity, the accuracy of the matrix measurements is reduced.

In Fig. 1, we show some of the different sample preparations that are used for OPASI-T. As described above, we use matrix methods to provide coverage at short wavelengths (KBr pellets and polyethylene disks are shown in Fig. 1). We require multiple matrix preparations because the embedding materials are transparent over limited wavelength ranges. At the shortest wavelengths, KBr and CsI both provide good transparency. KBr has a long wavelength cutoff of $\sim 25\,\mu$m, and CsI cuts off at $\sim 50\,\mu$m. Overlapping with both KBr and CsI, polyethylene provides access to wavelengths from $\sim 15\,\mu$m to very long wavelengths where the matrix samples cease to provide sufficient optical depth for high-quality measurements. To provide wavelength coverage from the near-IR to the far-IR, therefore, we require both matrix samples embedded in polyethylene and samples embedded in either KBr or CsI. For the majority of

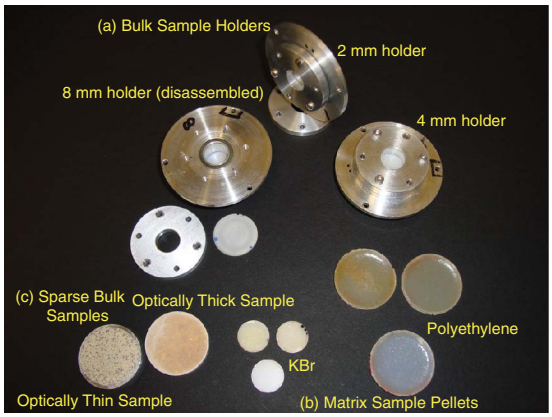

Fig. 1. (Color online) Many sample preparations are needed to cover the wide range in wavelengths. (a) Three bulk sample holders (8 mm, disassembled on the left, 2 mm on edge in the middle, and 4 mm at right), (b) KBr and polyethylene pellets used at short wavelengths, (c) bulk samples used for reflectivity measurements; a sparse, optically thin sample is on the left, with an optically thick sample on the right.

our measurements, we have chosen KBr rather than CsI, as CsI samples are more difficult to prepare and more expensive. Both KBr and CsI samples are hygroscopic and tend to degrade when exposed to the atmosphere; this requires careful storage of the samples. The use of KBr samples without supporting CsI samples does not lead to any limitations in our measurements, since the wavelength coverage of KBr and that of polyethylene overlap; CsI samples may still be prepared to complement the spectral range of the other preparations when necessary.

Each of the matrix preparations is prepared in a nearly identical way. For KBr and CsI disks, silicate condensate ($\leq \sim 1$ mg, with mass measured to ~0.0001 mg) is mixed and ground with 500 mg of the matrix material. This mixture is then pressed into a pellet under a pressure of 15000 psi. The pellets are 12.5 mm in diameter and approximately 1.5 mm thick. Polyethylene disks are prepared by mixing ~10–100 mg of silicate with 1000 mg of polyethylene beads. This mixture is melted in an aluminum mold to produce disks 25.4 mm in diameter and ~1.0 mm thick. Reference disks without silicate grains are similarly prepared for all matrix materials. A range of sample concentrations ensures that we have sufficient optical depth to obtain high signal-to-noise measurements of the sample material over the full wavelength range.

At longer wavelengths, we prefer to measure the samples in bulk form. This not only avoids the effect of the matrix material on the measured spectrum, but it also keeps the sample material itself intact. This is beneficial for both postmeasurement determination of the mass of the sample material and for microscopy of individual sample grains. Such bulk measurements are made possible because of the low opacity of the dust grains in this spectral regime. Depending upon the sample material, the opacity can drop rapidly as one moves to longer wavelengths; therefore, it is often necessary to use multiple sample holders of different thicknesses. The effective range for each sample holder is determined by the wavelength range where the transmission is between ~0.2 and ~0.8. Transmission values outside this range are more susceptible to uncertainties from reference samples and, therefore, are more vulnerable to systematic errors. The thinnest bulk-sample holder we have used is 2 mm thick and provides good coverage from ~100 μm out to ~350 μm for iron-rich silicate. The second is 4 mm thick and provides coverage from ~200 μm out to ~500 μm (iron-rich silicate); by contrast, this same holder provides coverage from ~100 μm to ~500 μm for our SiO_x samples (Fig. 2). Together, these holders provide overlapping measurements; the correlated measurements in the overlapping regions allow for normalization of data from different samples. We have also manufactured additional holders with thicknesses of 8, 12, 16, and 20 mm in case some samples require more sample material to achieve the necessary optical depth. The 8 mm holder has been used to provide wavelength coverage to ~1 mm for iron-rich silicates.

Transmission measurements of dust samples have traditionally been measured in the IR using an FTS. We use a Bruker IFS 113 v and IFS 125 hr FTS to provide transmission data for our samples. In conjunction with our array of sample holders, these instruments provide transmission data across the entire wavelength range. The Bruker IFS 113 v FTS is a dual interferometer system utilizing a Genzel interferometer to collect data in the mid- to far-IR (2–1000 μm) and a Michelson mode to collect data at short wavelengths (0.4–5.4 μm). The IFS 125 hr uses a modified Michelson interferometer (using a retroreflector instead of planar mirrors) to acquire data between 1–2000 μm. To obtain cryogenic transmission data, we insert an Oxford Optistat dynamic

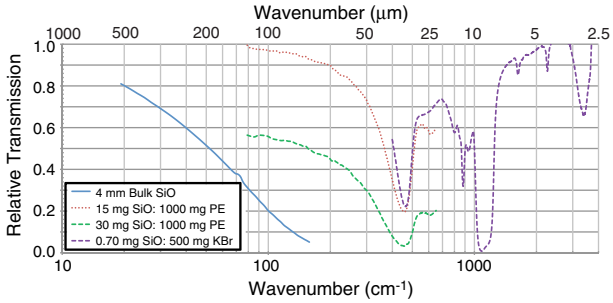

Fig. 2. (Color online) We have obtained data for SiO_x, covering a large spectral range by using our multiple sample preparations at multiple temperatures. By measuring a sample material with known properties, we are able to verify that each of our experiments is operating as expected. Here, we show SiO_x transmission data from FTS measurements, taken at room temperature (300 K). The four curves are for a 4 mm bulk SiO_x sample, two different densities of sample in a polyethylene (PE) matrix, and a sample prepared in a KBr matrix. Each sample preparation has a different optical depth; this allows us to obtain transmission values in the range of 0.2 to 0.8 as needed to determine the complex dielectric constant to high accuracy.

continuous flow cryostat with an Oxford ITC503 proportional-integral-derivative temperature controller in the optical path, allowing us to obtain data at temperatures ranging from 4.2 K to 300 K with up to ~0.2 K resolution. This is critical to provide the wide temperature range needed to explore the temperature dependence of dust spectra (Fig. 3).

In Fig. 4, we show the optical constants n and k for the polyethylene–SiO_x mixture, as calculated from the transmission data in Fig. 3. A clear shift in the index of refraction can be seen as the sample is cooled to 5 K from room temperature. The optical constants shown here are produced by using a model to fit the observed transmission data (see additional discussion in Section 4, "Sample Data for SiO_x"). The mean residual from the fit for the 30 mg sample in polyethylene is less than 0.01%, with a maximum residual of 1.25% at the low frequency end of the measurement. These small residuals imply that we are well able to fit the observed data; uncertainties are dominated by the accuracy of the transmission measurements themselves. We have made a statistical estimate of the uncertainties associated with our transmission measurements by examining a series of repeated measurements. We find that the mean uncertainty per point in our transmission spectrum is ~1%; the uncertainty can be up to a factor of a few larger where the transmission is low. Additional uncertainty can arise from sample preparation. In the case of embedded samples, we make multiple "identical" samples at the same time; when measured, however, these nominally identical samples can show transmission values that vary by ~2%. Again, however, the variation can be a factor of 2–3 larger in regions where the overall transmission is low.

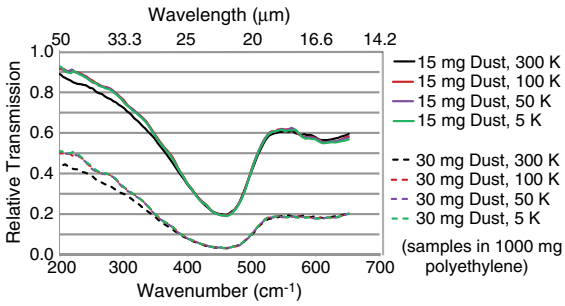

Fig. 3. (Color online) SiO_x, unlike many iron- and magnesium-rich condensates, does not show significant changes in spectrum with temperature. However, as shown here, there is a shift in the continuum transmission at long wavelengths. This demonstrates the need for measurements at different temperatures, even in this instance where the difference with temperature is relatively small. The OPASI-T program is designed to provide temperature resolution needed to probe temperature-dependent changes in the observed spectra. The two sets of curves shown here are for two different densities (15 mg with a filling fraction of 0.0056 and 30 mg with a filling fraction of 0.012) of sample material embedded in a polyethylene matrix; the same temperature behavior of the spectrum is seen in both samples.

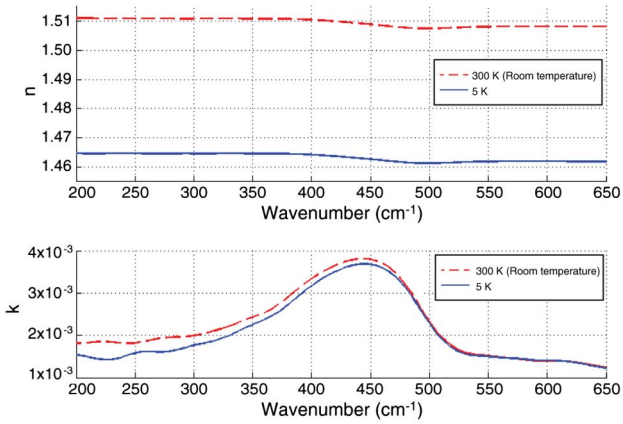

Fig. 4. (Color online) From the transmission data shown in Fig. 3, we have derived the n and k values for our SiO_x mixture embedded in polyethylene matrix (the results shown here are for the 30 mg sample with a filling fraction of 0.0119). The calculated values show clear differences between room temperature and 5 K.

B. Fourier Transform Spectrometer–Reflectometer Measurements

While transmission data provide significant insight into the properties of astronomically relevant materials, in order to accurately calculate the optical constants for these materials, we require additional data in the form of either scattering measurements or absorption (emissivity) measurements. In the OPASI-T program, we have built a new IR reflectometer to provide the complementary scattering/absorption measurements (Fig. 5) for wavelengths $>15\,\mu$m and at temperatures between 5 K and 100 K.

The integrating sphere itself is machined aluminum; the interior surface of the sphere is bead blasted with 16-grit silicon carbide, creating an approximately isotropic scattering surface, and gold-plated to maximize surface reflectivity. Light enters the sphere through a double-ended f/6 Winston cone; this provides illumination to a small patch (21.8 mm diameter) on the target. The input light can come either from a mercury lamp inside the Bruker IFS 113 v FTS or from a SiC ceramic light source. Three targets sit within a three-position sample wheel, allowing us to measure in sequence a "black" (absorptive) target, a reflective target, and the dust sample. All sample targets are deposited onto an aluminum substrate. Light reflected off the target then scatters inside the sphere to an f/2.44 Winston cone that brings the light to an IR Labs cooled germanium bolometer. This cone is positioned so that light from the sample cannot directly reflect from the sample into the detector Winston cone; this eliminates the need for baffling inside the sphere.

The sphere and bolometer are mounted to the cold plate of a liquid Helium cryostat. The sample wheel is thermally isolated from the cold plate with a stainless steel support bracket, with a mechanical heat switch to provide the ability to thermalize the wheel. Mounted to the wheel are both a thermometer and a 300 Ω resistive heater; the heater allows the wheel,

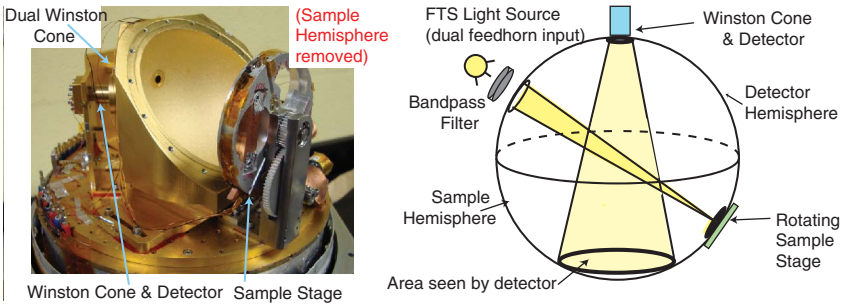

Fig. 5. (Color online) The reflectometer is designed to provide the complementary reflection and emission data needed to uniquely determine the complex dielectric constant for the sample material. On the right is a illustration of the design of the reflectometer; the hardware itself can be seen at left.

when isolated, to be temperature controlled between ~4.2 and ~100 K. Thermal radiation from the wheel provides the limit at the upper end of this scale, as when the wheel temperature exceeds 100 K, it radiatively heats the bolometer. Nevertheless, the thermal isolation and heater provide the range of temperatures needed for exploration of the sample properties. The wheel also has a magnetic switch that allows accurate tracking of the rotation position.

The IR reflectometer allows us to make the scattering and absorption measurements that complement the transmission data from the FTS and are needed in the calculation of the complex dielectric constants. If the dust sample is optically thick, then in the absence of scattering it would simply appear "black"; by comparing the data for a thick dust sample to that for our nonreflective sample, we measure scattering from the dust grains. If, on the other hand, the dust sample is optically thin, then the scattered light from the dust grains is observed in combination with the light transmitted through the sample and then scattered off the substrate. The difference between the thin sample and the reflective target, therefore, provides a measure of the absorption of the dust grains. One of the implications of this is that a given target sample has dual purpose. At short wavelengths, the target sample is optically thick, providing a measure of the scattering, while at long wavelengths, where the opacity of the sample has dropped significantly, it is optically thin and provides a measure of the absorptivity of the dust grains.

In Fig. 6, we show data acquired with our reflectometer for a SiO_x sample taken at 6 K. The sample used in this case is intermediate between optically thick and optically thin. This is not the ideal case for precise determination of the complex dielectric constant, but it serves our purpose here by showing the overall capability of the instrument. We have also acquired data with an optically thick sample at multiple temperatures. From this data, we are able to derive the reflectance of the SiO_x sample. The relatively low signal-to-noise necessary for reflection measurements limits the accuracy of our derived reflection values; as an example, we have measured a mean reflectance between 400 and 500 cm^{-1} (20 to 25 μm) of $4.8 \pm 1.9\%$; this corresponds to a local minimum in the reflection curve. Adjacent bands from 500 to 600 cm^{-1} and 300 to 400 cm^{-1} give mean reflectance of $5.4 \pm 0.9\%$ and $6.5 \pm 1.6\%$, respectively. Based upon repeated measurements, we estimate the uncertainty associated with individual points in our raw reflection measurements to be 2.7%.

One limitation of the reflectometer is that at present we are not able to observe short of 15 μm, due to the polyethylene film windows. Since we want to obtain data that covers the 10 μm silicate feature, we also use the built-in integrating sphere in the Bruker IFS 125 hr. Data from this experiment are shown in Fig. 7. The Bruker integrating sphere provides wavelength coverage over one full decade, from 2.5 to 25 μm. This overlaps with the range of our IR reflectometer, ensuring that we have full spectral coverage. We will continue, however, to push the spectral coverage of the reflectometer, ideally to provide coverage as short as 2.5 μm, eliminating the need to use two different apparatus to complete our data.

We also anticipate conversion of the reflectometer into an emissivitometer. In the emissivitometer configuration, we measure the thermal radiation from the sample itself. The sample is heated, and

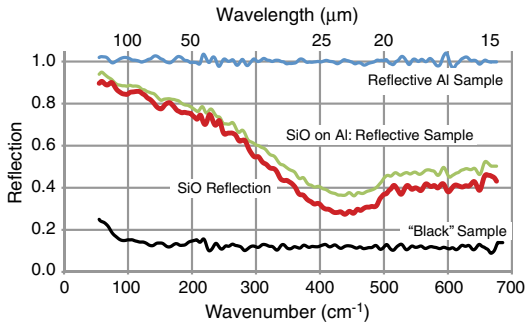

Fig. 6. (Color online) Our IR reflectometer allows us to obtain high-quality scattering data for optically thick target samples, while also providing the ability to measure absorptivity of optically thin samples. Here we show measurements taken with our reflectometer at 6 K for an optically thin SiO_x sample on an aluminum disk, along with the calibration measurements from a highly reflective aluminum sample and a "black," a corrugated nonreflective sample. The data shown is for a single run; noise within the data leads to localized values of the reflection coefficient that are greater than 1. Averages of multiple runs provide a measured reflection of ~0.99.

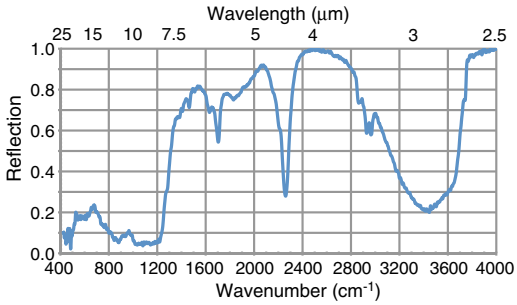

Fig. 7. (Color online) The IR reflectometer cannot yet obtain good quality data short of 15 μm, so we complement the wavelength coverage by using the room temperature integrating sphere on the Bruker IFS 125 hr in the near-IR and mid-IR. The data shown here are for the same SiO_x on Al sample as shown in Fig. 6.

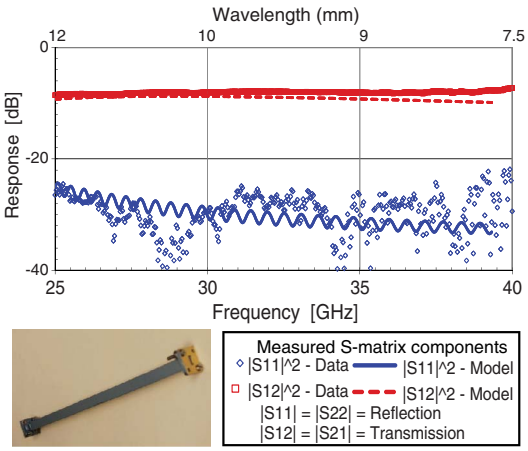

Fig. 8. (Color online) Using waveguide resonators (such as shown at bottom left) packed with an iron-rich sample, we derive the complex dielectric constant at submillimeter and millimeter wavelengths. The main panel shows measurements of the scattering matrix elements for material loosely packed into the waveguide with a filling fraction of 0.982. Models fit the data well; these models, combined with the knowledge of the filling factor of the material, allow accurate derivation of the dielectric constants.

IR photons from the warm sample are collected through the Winston cone. Following the Winston cone, the light continues onto a bolometer via a broadband filter (multiple filters are mounted within a single filter wheel to provide a wide range of spectral coverage). Technically, the data acquired with an emissivitometer is redundant, as only two of the three parameters (transmission, reflection, and emission) are needed to completely characterize the optical properties of a sample. However, the addition of emissivity measurements would provide a tool for further reducing the small residual systematic errors present in our current measurements.

C. Waveguide Measurements

At the longest wavelengths (longer than 800 microns), the samples appear essentially homogenous because the particle size is much smaller than the wavelength. This allows us to use a Fabry–Perot waveguide resonator technique to determine complex dielectric properties, using an HP 8510 network analyzer with WR28.0 waveguide flanges. This technique uses observations of the electromagnetic response from shims made of our sample material. These measurements provide a direct and precise determination of the dielectric properties of the materials at microwave and millimeter wavelengths (Fig. 8).

In Fig. 8, we show data acquired using our waveguide; the measurements are taken with the material loosely packed into the waveguide. In preparing the waveguide, the cavity is filled with the sample material, then lightly tapped to eliminate voids. This procedure is repeated in order to ensure that the waveguide is full and has relatively few voids. From the waveguide data, we extract the dielectric properties in the context of a Maxwell–Garnett mean field theory for a two-phase heterogeneous dielectric mixture [17]. From the WR28.0 waveguide Fabry–Perot resonance, we find an effective dielectric constant for the aggregate of $\varepsilon_r^* = 1.070 + 0.012i$ at a wavelength of 9 mm. Using the density of the sample within the waveguide ($0.0593\,g/cm^3$) relative to the density of the sample in bulk form ($3.32\,g/cm^3$), we calculate the iron silicate volume-filling fraction of 0.017. We then infer a bulk dielectric constant of $\varepsilon_r^* = 6.60 + 1.00i$ for the iron silicate material; this is the value of importance for modeling dust grain behavior. Notably, when compared to pure SiO, the sample has high loss but is consistent with previous measurements of fused silicate and alumina frits. We have not acquired data for our SiO_x mixture with this technique, as our instrumentation and methods have been previously demonstrated [18].

In this method, the sample thickness is critically important. Electrically thin samples with low loss provide information about the real component of the propagation constant, while thick samples provide information on the imaginary component. Therefore, to accurately derive the dielectric properties, we use two different shim thicknesses. The first provides several Fabry–Perot resonances over the 30% fraction waveguide band; the second is several e-folding lengths. From this rectangular waveguide data, we enforce causality following Baker-Jarvis [19] and derive the constitutive relations.

4. Sample Data for SiO_x

For a new program such as OPASI-T, it is important to have confidence in the operation and efficacy of the individual measurement systems. The millimeter-wave measurement techniques using waveguides have been demonstrated previously, but the reflectometer is all-new instrumentation, and the transmission measurements use a wide variety of new sample preparations. Therefore, we have acquired data using both the FTS transmission apparatus and the reflectometer for a silicon oxide mix (i.e., a mixture of SiO and SiO_2), as shown in the preceding sections. The SiO_x mixture is a glassy sample, with regions that are chemically more chaotic than a typical glass. The mixture can be approximated

stoichiometrically as $SiO_{1.5}$. The major advantage of using this material is that the optical properties of this material have been previously measured and we are able to compare our results against those in the literature. This is critical if we are to be confident in the results from our system.

In Fig. 9, we display values for the dielectric constant of our SiO_x mixture, calculated by employing a Lorenz model dielectric function for a two-component mixture (following Eq. 5.4 from [20]) to fit the measured transmission data. We also show comparison data from the literature for SiO and for KBr (the matrix material used in this wavelength range). Our results are consistent with the data in the existing literature [21,22]. It should be noted, however, that our materials are likely to have somewhat different characteristics than presented in [21], as the data shown there is for pure crystals. In particular, we expect our KBr pellets to have higher loss than the corresponding crystal, as crystal defects and voids within the material lead to additional absorption. For example, we have used our apparatus to measure a KBr-only pellet and derive $n = 1.508$ from the observed response; the value of n is in good agreement with [21]. In principle, we can also calculate the value of k, but with the current transmission data and the KBr's minimal loss, the uncertainty is relatively large. These results thus meet our expectation. The transmission spectrum derived from this modified Lorentz model has mean fitting residuals of ~0.25% relative to our measured transmission curves and a maximum residual of <1%. Our data reduction tools and analysis algorithms will be discussed in further detail in an upcoming paper [23].

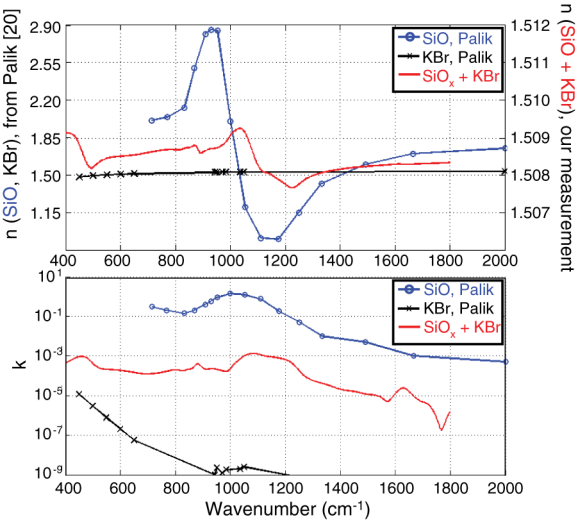

Fig. 9. (Color online) Based upon the measured transmission and reflection data from the OPASI-T experiments, we are able to calculate both components of the complex dielectric constant for our sample embedded in KBr (with a filling fraction of 9.8×10^{-4}). The results are consistent with previous measurements of the individual sample constituents; the KBr and SiO data shown above are from [21]. The results shown here (the SiO + KBr curve) are derived from room temperature transmission data.

5. Conclusions and Future Work

We have successfully demonstrated the efficacy of the OPASI-T instruments and measurement techniques, acquiring high-quality transmission and reflection data for SiO_x samples. From these data, we have calculated the optical constants, and the values determined from these measurements are in agreement with data available in the literature.

The OPASI-T program is now acquiring new data for both iron- and magnesium-rich silicates. The measurements cover a large span of wavelengths and temperatures, and we will also explore the effect of sample crystallinity on the observed spectrum. The optical constants determined from our data will be rapidly put to use by astronomers, leading to improved understanding of an array of astronomical phenomena (e.g., star formation, planet formation). In the future, we will continue our experiments to measure the optical properties of other astronomically relevant materials, including a variety of carbonaceous materials.

We will also explore additional improvements to the OPASI-T system. Further refinements of our sample holders and sample preparation may allow us to improve our overall processes for both the transmission measurements and the reflectometer. In addition, we will extend the wavelength coverage of both our reflectometer and the Bruker IFS 125 hr integrating sphere accessory. Our ultimate goal is to extend the coverage sufficiently that only measurements with the IR reflectometer are required. However, with the extended capabilities of the Bruker IFS 125 hr, we will be able to obtain additional data to demonstrate the repeatability of our measurements and to accurately assess systematic uncertainties within our reflectometer. Finally, we will complete the fabrication of hardware needed to use the reflectometer in an emissivitometer mode. In this mode, we will be able to directly measure the emission from a sample as a function of temperature, providing a redundant set of data that acts as a "check" on the results from our transmission and reflection measurements.

The material presented in this paper is based upon work supported by NASA Science Mission Directorate through the ROSES/APRA program. Additional support for this work was provided by NASA through the NASA Herschel Science Center Laboratory Astrophysics Program. Samples were prepared under support provided to J. Nuth by NASA's cosmochemistry program. R. Kinzer is supported by an appointment to the NASA Postdoctoral Program at Goddard Space Flight Center (GSFC), administered by the Oak Ridge Associated Universities under contract with NASA. Contributions to this project were also made by several students funded through NASA's Undergraduate Student Research Program (USRP): N. Lourie, J. Wheeler, N. Mihalko, and T. Chisholm. Laboratory support was also provided by Manuel Quijada in the Optics Branch at GSFC.

[§]USRA—Universities Space Research Association
[§]NASA Postdoctoral Program Fellow

References

1. N. J. Woolf and E. P. Ney, "Circumstellar infrared emission from cool stars," Astrophys. J. **155**, L181–L184 (1969).
2. R. Maas, E. Ney, and N. Woolf, "The 10-micron emission peak of comet Bennett 1969*i*," Astrophys. J. **160**, L101–L104 (1970).
3. E. van Dishoeck, "ISO spectroscopy of gas and dust: from molecular clouds to protoplanetary disks," Annu. Rev. Astron. Astrophys. **42**, 119–167 (2004).
4. F. Molster, L. Waters, and A. Tielens, "Crystalline silicate dust around evolved stars. II. The crystalline silicate complexes," Astron. Astrophys. **382**, 222–240 (2002).
5. N. Boudet, H. Mutschke, C. Nayral, C. Jäger, J.-P. Bernard, T. Henning, and C. Meny, "Temperature dependence of the submillimeter absorption coefficient of amorphous silicate grains," Astrophys. J. **633**, 272–281 (2005).
6. T. Henning and H. Mutschke, "Low temperature infrared properties of cosmic dust analogues," Astron. Astrophys. **327**, 743–754 (1997).
7. C. Kaito, Y. Ojima, K. Kamitsuji, O. Kido, Y. Kimura, H. Suzuki, T. Sato, T. Nakada, Y. Saito, and C. Koike, "Demonstration of crystalline forsterite grain formation due to coalescence growth of Mg and SiO smoke particles," Meteorit. Planet. Sci. **38**, 49–57 (2003).
8. S. L. Hallenbeck, J. A. Nuth III, and R. Nelson, "Evolving optical properties of annealing silicate grains: from amorphous condensate to crystalline mineral," Astrophys. J. **535**, 247–255 (2000).
9. K. L. Day, "Temperature dependence of mid-infrared silicate absorption," Astrophys. J. **203**, L99 (1976).
10. A. Zaikowsky, R. Knacke, and C. Porco, "On the presence of phyllosilicate minerals in the interstellar grains," Astrophys. Space Sci. **35**, 97–115 (1975).
11. H. Chihara, C. Koike, and A. Tsuchiyama, "Low-temperature optical properties of silicate particles in the far-infrared region," Publ Astron. Soc. Jpn. **53**, 243–250 (2001).
12. T. Henning and H. Mutschke, "Optical properties of cosmic dust analogs: a review," J. Nanophoton. **4**, 041580 (2010).
13. A. Tamanai, H. Mutschke, J. Blum, Th. Posch, C. Koike, and J. Ferguson, "Morphological effects on IR band profiles. Experimental spectroscopic analysis with application to observed spectra of oxygen-rich AGB stars," Astron. Astrophys. **501**, 251–267 (2009).
14. F. J. M. Rietmeijer, J. A. Nuth, and J. M. Karner, "Metastable eutectic condensation in a Mg-Fe-SiO-H2-O2 vapor: Analogs to circumstellar dust," Astrophys. J. **527**, 395–404 (1999).
15. S. Rinehart, D. Benford, E. Dwek, R. Henry, R. Silverberg, and E. Wollack, "Optical properties of astronomical silicates," Proc. SPIE **7014**, 70142G (2008).
16. R. E. Kinzer Jr., S. Rinehart, D. Benford, E. Dwek, R. Henry, J. Nuth, R. Silverberg, C. Wheeler, and E. Wollack, "Optical properties of astronomical silicates with infrared techniques," Proc. SPIE **7741**, 774128 (2010).
17. G. A. Niklasson, C. G. Granqvist, and O. Hunderi, "Effective medium models for the optical properties of inhomogeneous materials," Appl. Opt. **20**, 26–30 (1981).
18. E. J. Wollack, D. J. Fixsen, R. Henry, A. Kogut, M. Limon, and P. Mirel, "Electromagnetic and thermal properties of a conductively loaded epoxy," Int. J. Infrared Millim. Waves **29**, 51–61 (2008).
19. J. Baker-Jarvis, R. G. Geyer, and P. D. Domich, "A nonlinear least-squares solution with causality constraints applied to transmission line permittivity and permeability determination," IEEE Trans. Instrum. Meas. **41**, 646–652 (1992).
20. G. Kristensson, S. Rikte, and A. Sihvola, "Mixing formulas in the time domain," J. Opt. Soc. Am. A **15**, 1411–1422 (1998).
21. E. Palik, *Handbook of Optical Constants of Solids* (Elsevier, 1998).
22. G. Hass and C. Salzberg, "Optical properties of silicon monoxide in the wavelength region from 0.24 to 14.0 microns," J. Opt. Soc. Am. **44**, 181–183 (1954).
23. R. E. Kinzer Jr., S. Rinehart, D. Benford, G. Cataldo, J. Nuth, R. Silverberg, and E. Wollack, "Measured dielectric constants for iron-rich silicate smokes in the far-infrared," Astrophys. J. (to be published).